Cortical waves and post-stroke brain stimulation

Nikolai Bessonov, Anne Beuter, Sergei Trofimchuk, Vitaly Volpert

Cortical waves and post-stroke brain stimulation

Nikolai Bessonov[1], Anne Beuter[2], Sergei Trofimchuk[3], Vitaly Volpert[4,5,6,7]

[1]Institute of Problems of Mechanical Engineering, Russian Academy of Sciences, Saint Petersburg 199178, Russia

[2]Bordeaux INP, Bordeaux, France, Equipage Innovation SARL, Plérin, France

[3]Instituto de Matematica y Fisica, Universidad de Talca, Talca, Casilla 747, Chile

[4]Institut Camille Jordan, UMR 5208, CNRS, University Lyon 1, Villeurbanne, 69622, France

[5]INRIA Team Dracula, INRIA Lyon La Doua, Villeurbanne 69603, France

[6]Peoples Friendship University of Russia, (RUDN University), 6 Miklukho-Maklaya, St Moscow 117198, Russian Federation

[7]Marchuk Institute of Numerical, Mathematics of the RAS, ul. Gubkina 8, Moscow 119333, Russian Federation

Funding information
RUDN University Program 5-100,
Grant/Award Number: RSF grant number
18-11-00171; The French-Russian project,
Grant/Award Number: PRC2307

A neural field model with different activation and inhibition connectivity and response functions is considered. Stability analysis of a homogeneous in space solution determines the conditions of the emergence of stationary periodic solu-tions and of periodic travelling waves. Various regimes of wave propagation are illustrated in numerical simulations. The influence of external stimulation on the wave properties is investigated.

KEYWORDS

brain stimulation, integro-differential equation, neural field model, waves

1 | INTRODUCTION

Over the last few years, there has been an increasing interest in the application of noninvasive stimulation such as Repetitive transcranial magnetic stimulation (TMS), Transcranial random noise stimulation (tRNS), Transcranial alternating current stimulation (tACS), Transcranial direct current stimulation (tDCS) (see Vosskuhl et al[1]), or minimally invasive brain stimulation such as cortical electrical stimulation[2] to treat a variety of neurologic and psychiatric conditions. This growing interest is probably due in part to an increasing understanding of the physiological control mechanisms driving normal and abnormal structural and functional brain reorganization. Specifically, these mechanisms are actively explored for stroke[3-5] and for post stroke aphasia,[6,7] to name a few. Recent studies on detailed mapping of the healthy and diseased brain connectivity shed new light on the relation between brain structure and function.[8] Today, brain con-

nectivity and brain dynamics are combined in an integrated framework.[9] An interesting observation regarding brain dynamics is that oscillations at multiple frequencies form spatially continuous neural patterns such as travelling waves. They are defined as a spatially coherent oscillation that propagates progressively across the cortex with known amplitude, frequency, and speed.[10] These travelling waves are functionally important for human behaviors such as perception, action, and language.[11,12] Propagation of alpha waves in the neocortex is studied in Bahramisharif et al[13] and Patten et al.[14] Travelling waves in the visual cortex are investigated in Sato et al[15] and in motor cortex in Takahashi et al.[16]

In the presence of brain disorders, these waves become disorganized and brain networks become disconnected or deactivated. But controlling dynamics in neural systems via brain stimulation techniques remains challenging because as indicated by Tang and Bassett,[17] "While some understanding has been gained of the control of single neurons, the control of large scale neural systems networks of multiply interacting components remains poorly understood." As a result, in most cortical stimulation protocols, be they electric or magnetic, parameter values are still adjusted in an empirical fashion. Despite this limitation, cortical stimulation studies clearly produce encouraging results suggesting that these techniques have some potential, but overall, the results remain mixed or limited for example for stroke (see previous studies[18-23]), with improvements sometimes limited[24] to 10% to 20%, and for post-stroke aphasia (see other works[25-30]). Aphasia is a complex brain disorder of language and communication caused by damage to the language networks affecting speaking, reading, writing, or understanding language.

In order to propose more efficient stimulation protocols in the future, it is important to predict the dynamics of the propagating waves, to detect deviant values of propagating wave parameters (ie, wave speed, amplitude, and frequency) and to identify the precise localization of the nodes to be stimulated. These constraints imply the use of bio-inspired modeling tools to reconstruct the information content of the propagating wave and to monitor in time and space the stimulation to be introduced via a closed-loop control system to compensate for the disruption. Until now, this type of cortical stimulation was not available.

However, things may change soon for two reasons. The first reason is that the focus of research has progressively shifted from examining specific brain regions to exploring specific brain networks.[31,32] The challenge to treat brain networks is to understand and control the brain's capacity to reorganize itself.[7] The second reason is that it is now possible to describe cortical waves mathematically with increasing precision.[10,33,34] These recent modeling studies are opening the possibility to harness the brain's capacity to reorganize itself with the help of an outside stimulation introduced only when and where necessary. Thus, it may soon become possible to restore or repair interacting brain networks with the consequence of improving significantly symptoms associated with a variety of brain disorders affecting most components of human behaviors (action, emotion, and cognition).

By definition, every model is a simplification of reality, but an effort is made to render the model realistic neurophysiologically. For example, we incorporate the effect of the extracellular field on the transmembrane potential of neurons (ie, ephaptic coupling, Appendix A). In addition, the model distinguishes activation and inhibition response functions, it differentiates short range activation and long range inhibition, its connectivity function is asymmetric.

In the present paper, we study the propagation of waves of electric potential in the cortical tissue with integro-differential equations arising in neural field models. The main motivation of this work is to study the propagation of brain waves in the normal and in the damaged tissue and to show that external stimulation can restore the properties of the waves altered by the tissue damage. We will consider different stimulation techniques and will discuss the conditions of their applicability. Stability analysis presented in Section 3 will allow us to determine conditions of appearance of stationary spatial structures and of periodic travelling waves. Different regimes of wave propagations are illustrated in Section 4. The question of the response to electric stimulation for different stimulation types is addressed in Section 5. We conclude this work by a discussion of the model and of the results and by future perspectives.

2 | MODEL

We consider the equation for the local density $u(x, t)$ of activated (firing) neurons as a function of space point x and time t:

$$\frac{\partial u}{\partial t} = D\Delta u + g(K - u)H(W_a) - g(u)H(W_i) - \sigma u. \tag{2.1}$$

The first term in the right-hand side of this equation describes neuron activation due to ion diffusion through the extracellular matrix, direct gap junction communication, and ephaptic effects[35] (see Section 6). On the other hand, electrodynamic effects (second time derivative) are not taken into account. The second and third terms take into account neuron activa-

tion and deactivation by signals coming from other neurons along axons. Instead of activating and inhibitory neurons in Wilson and Cowan,[36] we consider here a single group of neurons with activating W_a and inhibitory W_i signals. This group of neurons can be interpreted as ensemble of activating and inhibitory neurons sending different types of signals. The last term describes intrinsic deactivation rate, that is, not related to the inhibition signals.

We denote by K the total neuron density, so that $K - u$ is the density of inactivated neurons. In the linear approximation, the product $(K - u)W_a$ determines the rate of neuron activation by the activating signal W_a. In a more general setting, we take into account saturation with respect to the neuron density and the force of activation signal by the introduction of some growing non-negative functions $g(u)$ and $H(W)$. Thus, $g(K - u)H(W_a)$ is the rate of neuron activation and $g(u)H(W_i)$ is the rate of their deactivation.

The activating signal is the electric potential produced by other neurons and coming to the given space point x along the axons. It can be considered in the form[37]:

$$W_a(x,t) = \int_\Omega \phi_a(x,y) S_a\left(u\left(y, t - \frac{|x-y|}{q_a}\right)\right) dy. \tag{2.2}$$

This expression describes the intensity of signal coming from all points y in the spatial domain Ω to the point x. Here, $S_a(u)$ is the excitation generation (response function) produced by activated neurons, q_a is the excitation speed, $|x-y|/q_a$ is the time delay due to the excitation propagation from the point y to the point x, and $\phi_a(x,y)$ is the connectivity function. The inhibitory signal has a similar form,

$$W_i(x,t) = \int_\Omega \phi_i(x,y) S_i\left(u\left(y, t - \frac{|x-y|}{q_i}\right)\right) dy \tag{2.3}$$

with possibly different functions ϕ_i and S_i. Equation 2.1 with expressions (2.2), (2.3) represents a closed model for the density of activated neurons.

Connectivity functions $\phi_a(x,y)$ and $\phi_i(x,y)$ characterize the density and the length of axons connecting the neurons. Let us note that signals in axons propagate only in the direction of their terminals. Therefore, signal propagation is not in general symmetric: it can be different from y to x and from x to y (see Section 6). It depends on the number and on the direction of connections between the two points. Connectivity functions are often considered as exponential functions of the distance $r = x - y$[37,38]:

$$\phi_a(r) = \begin{cases} a_1 e^{-b_1 r}, & r > 0 \\ a_3 e^{b_3 r}, & r < 0 \end{cases}, \quad \phi_i(x) = \begin{cases} a_2 e^{-b_2 r}, & r > 0 \\ a_4 e^{b_4 r}, & r < 0 \end{cases}, \tag{2.4}$$

where a_i, b_i are some positive constants. In this work, we use the functions ϕ_a and ϕ_i defined in (2.4) unless otherwise is stated.

Response functions $S_a(u)$ and $S_i(u)$ are non-negative nondecreasing functions usually considered as sigmoid functions, that is, they have an interval of rapid growth followed by saturation (Figure A1).Their exact form will be specified below.

If both densities u and $K - u$ are sufficiently large, then the function g is close to its saturation value. On the other hand, if the signals W_a and W_i are sufficiently small, then the function $H(W)$ can be approximated by a linear function. In this case, we obtain the equation

$$\frac{\partial u}{\partial t} = D\Delta u + W_a(x,t) - W_i(x,t) - \sigma u, \tag{2.5}$$

where the constant factors are omitted for simplicity of notation. The variable u in Equation 2.5 can be interpreted as the electric potential and not the density of activated neurons. Although these variables are related to each other and, in the first approximation, they can be considered as linearly correlated, there is a difference between them which should be taken into account. Clearly, the density of neurons cannot become negative, while the electric potential can have variable sign. In both cases, we can interpret the variable u as a deviation from an equilibrium neuron density or electric potential in the linearized model[37] in such a way that this variable can change sign.

Various particular cases of this equation were considered in the literature. The case without diffusion ($D = 0$) and without inhibition term ($\phi_i(x,y) \equiv 0$) was considered in Ermentrout and McLeod[39] as a model of neural network. A slightly modified equation was considered to describe thalamic waves.[40] A similar equation with both activation and inhibition connectivity functions was considered in Modolo et al[37] to model brain stimulation in the case of Parkinson's disease. The case with diffusion but without inhibition was studied in Bessonov et al[33] and Beuter et al.[34]

In the remaining part of the work, we will study Equation 2.5 in the limit of large excitation speed q where the time delay $|x - y|/q$ disappears. The case with time delay will be studied in the subsequent works.

3 | STABILITY ANALYSIS

In the limiting case of large excitation speed, $q = \infty$, and in the 1D case ($\Omega = \mathbb{R}$), Equation 2.5 writes:

$$\frac{\partial u}{\partial t} = D\frac{\partial^2 u}{\partial x^2} + \int_{-\infty}^{\infty} (\phi_a(x-y)S_a(u(y,t)) - \phi_i(x-y)S_i(u(y,t)))\,dy - \sigma u. \tag{3.1}$$

Homogeneous in space stationary solution $u = u_0$ of this equation is a solution of the equation

$$F(u) \equiv \phi_a^0 S_a(u) - \phi_i^0 S_i(u) - \sigma u = 0, \tag{3.2}$$

where

$$\phi_a^0 = \int_{-\infty}^{\infty} \phi_a(x)dx, \quad \phi_i^0 = \int_{-\infty}^{\infty} \phi_i(x)dx.$$

Linearizing Equation 3.1 about u_0 and applying the Fourier transform, we get the expression for the spectrum:

$$\lambda(\xi) = -D\xi^2 + s_a\tilde{\phi}_a(\xi) - s_i\tilde{\phi}_i(\xi) - \sigma, \tag{3.3}$$

where $s_a = S_a'(u_0), s_i = S_i'(u_0)$, $\tilde{\phi}_a(\xi)$ and $\tilde{\phi}_i(\xi)$ are the Fourier transforms of the corresponding functions. The variable ξ adopts all real values if we consider the whole axis and some discrete set of values for a bounded interval (say, $[0, L]$) with the periodic boundary conditions.

Suppose that $\lambda(0) = F'(u_0) < 0$, where the function $F(u)$ is defined in (3.2). Then in the narrow connectivity limit, where the functions ϕ_a and ϕ_i are replaced by the δ-function and the integral term in Equation 3.1 is replaced by $\phi_a S_a(u), \phi_i S_i(u)$, the homogeneous in space stationary solution $u = u_0$ is asymptotically stable. We will verify whether $\lambda(\xi)$ can have a positive real part for other real values of ξ providing instability of the solution u_0. We have

$$\begin{aligned}
\tilde{\phi}_a(\xi) &= \int_{-\infty}^{\infty} \phi_a(x)e^{ix\xi}dx = \int_{-\infty}^{\infty} \phi_a(x)\cos(\xi x)dx + i\int_{-\infty}^{\infty} \phi_a(x)\sin(\xi x)dx \\
&= \frac{a_1 b_1}{b_1^2+\xi^2} + \frac{a_3 b_3}{b_3^2+\xi^2} + i\xi\left(\frac{a_1}{b_1^2+\xi^2} - \frac{a_3}{b_3^2+\xi^2}\right), \\
\tilde{\phi}_i(\xi) &= \frac{a_2 b_2}{b_2^2+\xi^2} + \frac{a_4 b_4}{b_4^2+\xi^2} + i\xi\left(\frac{a_2}{b_2^2+\xi^2} - \frac{a_4}{b_4^2+\xi^2}\right).
\end{aligned}$$

3.1 | Activation without inhibition

If $\phi_i(x) \equiv 0$, then Re $\lambda(\xi) \le \lambda(0) < 0$ for all real ξ. Therefore, the homogeneous in space solution u_0 is stable.

3.2 | Symmetric connectivity functions

Suppose that

$$a_1 = a_3, b_1 = b_3, a_2 = a_4, b_2 = b_4. \tag{3.4}$$

Then,

$$\tilde{\phi}_a(\xi) = \frac{2a_1 b_1}{b_1^2+\xi^2}, \quad \tilde{\phi}_i(\xi) = \frac{2a_2 b_2}{b_2^2+\xi^2}.$$

Suppose that

$$s_a\tilde{\phi}_a(0) < s_i\tilde{\phi}_i(0) \text{ and } s_a\tilde{\phi}_a(\xi) > s_i\tilde{\phi}_i(\xi) \text{ for some } \xi. \tag{3.5}$$

The first condition is satisfied if $s_a a_1 b_2 < s_i a_2 b_1$, and it implies that $\lambda(0) < 0$. The second condition is satisfied if

$$(s_a a_1 b_1 - s_i a_2 b_2)\xi^2 > b_1 b_2(s_i a_2 b_1 - s_a a_1 b_2).$$

Since the right-hand side of this inequality is positive, then it can be satisfied for some ξ if and only if $s_a a_1 b_1 > s_i a_2 b_2$. We can now formulate the following assertion.

Proposition 3.1. *Suppose that the following inequalities are satisfied:*

$$\frac{b_1}{b_2} > \frac{s_a a_1}{s_i a_2}, \quad \frac{b_1}{b_2} > \frac{s_i a_2}{s_a a_1}. \tag{3.6}$$

Then properties (3.5) hold.

It follows from conditions (3.6) that $b_1 > b_2$. Hence, the activation connectivity function decays faster than inhibition connectivity function. This condition can be formulated as short range activation long range inhibition, similar to the case of Turing instability. Under the conditions of Proposition 3.1, solution u_0 becomes unstable for D and σ sufficiently small.

We recall that stability boundary is determined by the values of parameters for which the maximal real part of the spectrum lies at the imaginary axis. Setting $\lambda(\xi) = 0$ in (3.3), we get σ as a function of ξ at the stability boundary:

$$\sigma = \frac{2s_a a_1 b_1}{b_1^2 + \xi^2} - \frac{2s_i a_2 b_2}{b_2^2 + \xi^2} - D\xi^2 \equiv \Phi_1(\xi). \tag{3.7}$$

Figure 1 (left) shows two examples of the stability boundary. The upper curve has positive values in some interval of frequencies ξ. For the values of σ less than the maximum of this function, the maximal eigenvalue is positive leading to the emergence of a periodic in space solution (Figure 1, right). The lower curve is nonpositive. Therefore, the emergence of periodic solutions cannot be observed. Since the maximum of this function equals zero, it separates the cases with and without instability.

Let us recall that in the case of a bounded interval, we have a discrete set of values $\xi_j = 2\pi j/L, j = 1, 2, \ldots$. The instability occurs if $\sigma < \Phi_1(\xi_j)$ for some j. If this condition is satisfied for more than one value of j, then solutions with different frequencies can bifurcate.

The maximum of the bifurcating solution as a function of σ is shown in the bifurcation diagram (Figure 2). We observe a typical square root dependence near the bifurcation point. It is interesting to note that amplitude growth accelerates for further decrease of σ.

3.3 | Asymmetric connectivity functions

Suppose now that conditions (3.4) are not satisfied. In this case, the eigenvalue (3.3) has a nonzero imaginary part. Set $\lambda(\xi) = \alpha(\xi) + i\beta(\xi)$, where

$$\begin{aligned}
\alpha(\xi) &= \frac{s_a a_1 b_1}{b_1^2 + \xi^2} + \frac{s_a a_3 b_3}{b_3^2 + \xi^2} - \frac{s_i a_2 b_2}{b_2^2 + \xi^2} - \frac{s_i a_4 b_4}{b_4^2 + \xi^2} - D\xi^2 - \sigma, \\
\beta(\xi) &= s_a \xi \left(\frac{a_1}{b_1^2 + \xi^2} - \frac{a_3}{b_3^2 + \xi^2} \right) - s_i \xi \left(\frac{a_2}{b_2^2 + \xi^2} - \frac{a_4}{b_4^2 + \xi^2} \right).
\end{aligned} \tag{3.8}$$

As before, the stability boundary is given by the condition $\alpha(\xi) = 0$:

$$\sigma = \frac{s_a a_1 b_1}{b_1^2 + \xi^2} + \frac{s_a a_3 b_3}{b_3^2 + \xi^2} - \frac{s_i a_2 b_2}{b_2^2 + \xi^2} - \frac{s_i a_4 b_4}{b_4^2 + \xi^2} - D\xi^2 \equiv \Phi_2(\xi). \tag{3.9}$$

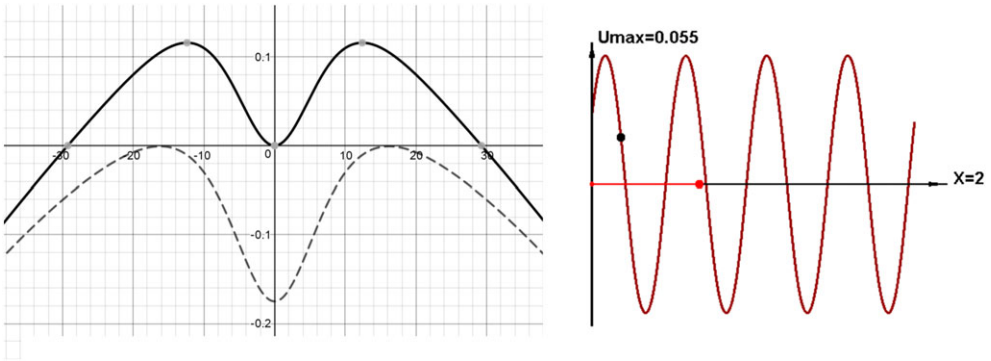

FIGURE 1 Function $\Phi_1(\xi)$ for two different sets of parameters (left) and a stationary periodic in space solution bifurcating from the homogeneous in space solution (right). The red interval on the x-axis is used to introduce a perturbation of the homogeneous solution, the black dot at the curve is used to measure the speed of travelling waves [Colour figure can be viewed at wileyonlinelibrary.com]

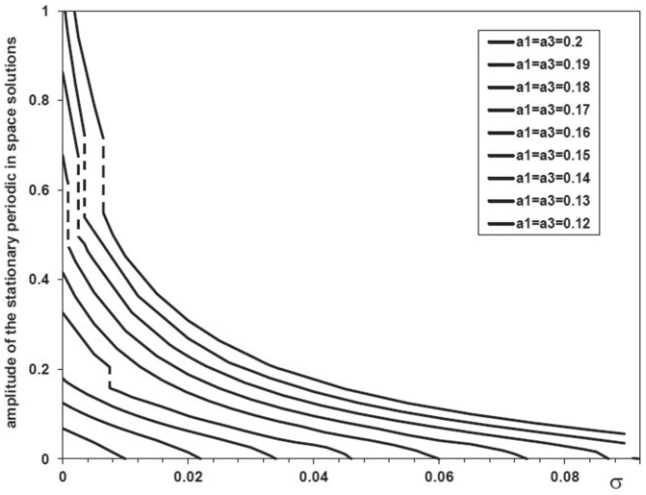

FIGURE 2 Bifurcation diagram: the amplitude of the stationary periodic in space solutions obtained in numerical simulations as a function of σ for different values of a_1 and a_3. The curves ordered according to the values of parameters given in the inserted box from the top to the bottom. Dashed lines show the transitions between the solutions with different periodicity. Other values of parameters are given in the Appendix A

The instability occurs if $\sigma < \Phi_2(\xi)$ for some values of ξ. Since there are two complex conjugate eigenvalues $\lambda(\xi) = \alpha(\xi) \pm i\beta(\xi)$, then at the stability boundary $\alpha = 0$ the bounded solution of the linearized equation writes

$$u(x,t) = e^{i\beta t}e^{i\xi x} + e^{-i\beta t}e^{-i\xi x} = \cos(\beta t + \xi x).$$

Here, ξ is found from the equation $\alpha(\xi) = 0$ and β is given by equality (3.8). This solution represents a periodic wave with frequency ξ and speed $c = -\beta/\xi$. We get from (3.8):

$$c = -s_a\left(\frac{a_1}{b_1^2+\xi^2} - \frac{a_3}{b_3^2+\xi^2}\right) + s_i\left(\frac{a_2}{b_2^2+\xi^2} - \frac{a_4}{b_4^2+\xi^2}\right). \tag{3.10}$$

If there are two (or more) different frequencies ξ_1 and ξ_2 satisfying the condition $\sigma < \Phi(\xi_j), j = 1, 2$, then there are two waves with different speeds and frequencies. According to (3.10), the value of the speed can increase with frequency or decrease depending on the values of parameters.

4 | REGIMES OF WAVE PROPAGATION

4.1 | Monotone waves

Replacing the connectivity functions ϕ_a and ϕ_i by the δ-function, we obtain conventional reaction-diffusion equation

$$\frac{\partial u}{\partial t} = D\frac{\partial^2 u}{\partial x^2} + S_a(u) - S_i(u) - \sigma u. \tag{4.1}$$

For the typical functions $S_a(u)$ and $S_i(u)$ (Figure A1), the function $f(u) = S_a(u) - S_i(u) - \sigma u$ has three non-negative zeros, u_+, u_0, u_-, $u_+ < u_0 < u_-$ if σ is less than some critical value σ_c. In this case, there is a travelling wave solution of this equation, that is, a solution $u(x,t) = w(x - ct)$ with the limits $w(\pm\infty) = u_\pm$ (see Volpert[41] and the references therein). This wave is a monotonically decreasing function of x, and it is globally asymptotically stable. The wave speed c admits various estimates and representations.

If the activation connectivity function ϕ_a has a finite support and the inhibitory connectivity function identically equals zero, $\phi_i(x) \equiv 0$, then, as before, there exists a monotone wave solution of equation (3.1). Its existence and stability can be studied by conventional methods based on the maximum principle.[42-44] Its speed is investigated in Bessonov et al[33] and Beuter et al.[34] Finally, if both connectivity functions are present and they have bounded supports, existence and stability of waves with the limits $w(\pm\infty) = u_\pm$ are not studied analytically since the existing methods are not applicable. We can

expect their existence and stability in the case where the homogeneous in space solution u_- is stable (Section 3). Example of numerical simulations of such waves is shown in Figure 3 (left).

4.2 | Time-periodic waves

If the homogeneous in space stationary solution u_- becomes unstable, then a stationary periodic in space solution bifurcates from it. In the case of wave propagation, this periodic structure emerges behind the wave. Thus, we have two propagating solutions: the wave from u_+ to u_- and the transition from u_- to the periodic in space stationary solution. Depending on their speeds, they can either propagate one after another or they can merge. An example of such transition is shown in Figure 3 (right) for the response functions $S_a(u) = S_i(u) = \arctan(hu)$ (the values of parameters are given in the Appendix A). Here, the solution $u = 0$ is unstable, and we observe a transition from the unstable homogeneous in space solution to the stable periodic in space structure. This transition propagates as a time periodic travelling wave.

4.3 | Stationary periodic waves

Stability analysis carried out in Section 3 shows the existence of eigenvalues with a nonzero imaginary part in the case of asymmetric connectivity functions. The corresponding eigenfunctions have the form $\cos(\beta t + \xi x)$. These are waves with the spatial frequency ξ and the speed $-\beta/\xi$. They are observed in numerical simulations (Figure 4).

4.4 | Other regimes

Stationary periodic waves can become unstable leading to the appearance of modulated waves. In this case, the spatial frequency remains constant but the amplitude of spatial oscillations is a periodic function itself. In the example shown in Figure 5 (left), the periodic wave propagates to the right and the modulation wave propagates to the left.

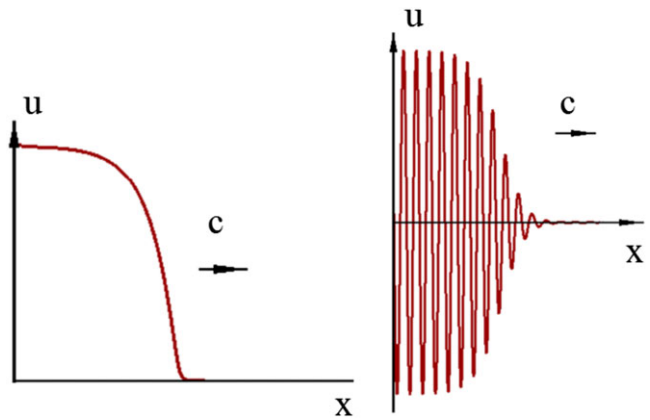

FIGURE 3 Snapshots of a monotone wave (left) and of a wave with a stationary periodic structure behind it (right) [Colour figure can be viewed at wileyonlinelibrary.com]

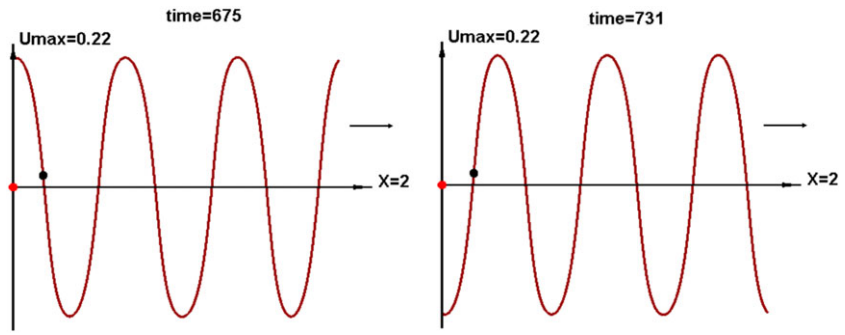

FIGURE 4 Snapshots of the periodic wave. It is a periodic in space solution moving with a constant speed. The function in the right figure can be obtained from the function in the left figure by a shift on half-period [Colour figure can be viewed at wileyonlinelibrary.com]

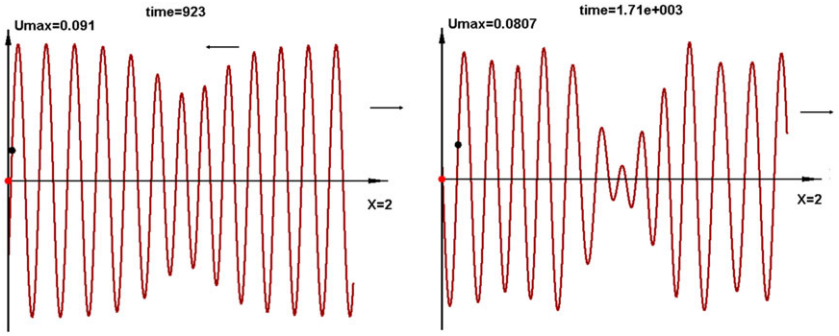

FIGURE 5 Snapshots of periodic waves with a periodically modulated amplitude (left) and with aperiodic amplitude modulation (right). The wave of amplitude modulation moves in the direction opposite to the direction of the periodic wave [Colour figure can be viewed at wileyonlinelibrary.com]

For other values of parameters, the modulation of the amplitude loses its periodicity, and more complex propagating solutions are observed (Figure 5, right). Their spatial frequency remains approximately constant while the amplitude has aperiodic oscillations.

5 | METHODS OF STIMULATION

5.1 | Constant activation

In the case of monotone waves, the wave speed can change in the damaged tissue because the connectivity and response functions are different in comparison with the normal tissue. We studied the influence of constant stimulation I on the speed of wave propagation in Bessonov et al[33] and Beuter et al.[34] It is shown that under some conditions, it is possible to restore the speed of wave propagation by the stimulation. These conditions are formulated in terms of the relative properties of the normal and damaged tissues.

5.2 | Linear activation

We call the stimulation $I = ku$ linear activation since additional activating signal is linearly proportional to the observed potential in the tissue. Hence, the same electrode measures electric potential in the cortex and sends stimulating signal depending on the measured signal. In this case, we replace the intrinsic inhibition rate σ by $\sigma - k$. Let us recall that in the case of periodic waves, the wave frequency ξ should satisfy the condition $\sigma < \Phi_2(\xi)$. This condition may not be satisfied for the damaged tissue since the connectivity and response parameters a_i, b_i, s_a, s_i can have lesser value for the damaged tissue than for the normal tissue. Denote by $\Phi_2^*(\xi)$ the corresponding function for the damaged tissue. If the condition $\sigma < \Phi_2^*(\xi)$ is not satisfied but $\Phi_2^*(\xi) > 0$, we can choose such k that $\sigma - k < \Phi_2^*(\xi)$. Hence, we can restore the same frequency of wave propagation. However, the wave speed c in (3.10) does not depend on σ. Therefore, we cannot restore the wave speed by this method of stimulation.

5.3 | Periodic activation

Due to decrease of the connectivity and response functions in the damaged tissue, periodic waves can completely disappear resulting in stability of the homogeneous in space stationary solution. Stability condition in the damaged tissue holds if $\sigma > \Phi_2^*(\xi)$ for all ξ. In this case, the periodic stimulation $I = I_0 \cos(px + qt)$ with properly chosen p and q provides periodic waves with the corresponding frequency p and speed $-q/p$.

This approach can be applied in the case where the homogeneous in space stationary solution is unstable and the resulting spatial solution has a sufficiently small amplitude. Then for a strong enough stimulation function, we get the solution with the desired speed and frequency modulated by weak amplitude oscillations (Figure 6). The same stimulation applied to low amplitude modulated waves (Figure 5) gives the same result as in Figure 6 (right).

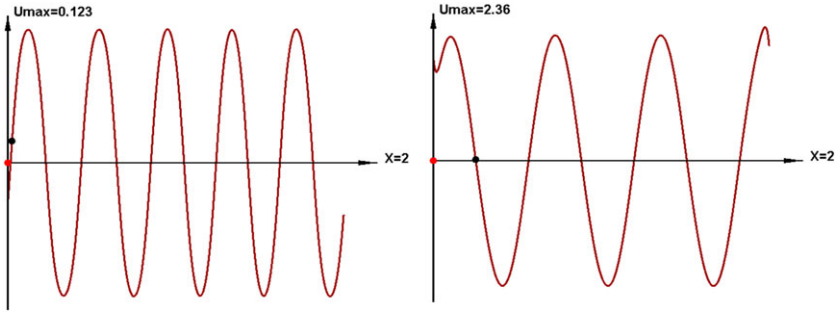

FIGURE 6 A stationary periodic in space solution (left). Applying the stimulation function $I = I_0 \cos(px + qt)$, we get a solution close to a periodic wave with a weakly oscillating amplitude. The spatial frequency and the speed of propagation are determined by the parameters p and q of the stimulation function [Colour figure can be viewed at wileyonlinelibrary.com]

5.4 | Linear deactivation and periodic activation

The periodic stimulation considered above is efficient if remaining intrinsic waves in the damaged tissue have sufficiently small amplitude and they do not perturb the stimulation. If this is not the case, we can impose, first, inhibiting stimulation $I_1 = -ku$ in order to suppress remaining oscillations. The second stimulation $I_2 = I_0 \cos(px + qt)$ will allow the reconstruction of desired wave frequency and speed. Thus, the total stimulation $I = I_1 + I_2$ consists of two parts indicated above.

5.5 | Complete signal reconstruction

Signal propagation can be different in the normal and in the damaged tissues since their properties differ from each other. Let us write Equation 2.1 for the normal tissue

$$\frac{\partial u}{\partial t} = D\frac{\partial^2 u}{\partial x^2} + g(K-u)H(W_a^{(1)}(u)) - g(u)H(W_i^{(1)}(u)), \tag{5.1}$$

and

$$\frac{\partial v}{\partial t} = D\frac{\partial^2 v}{\partial x^2} + g(K-v)H(W_a^{(2)}(v)) - g(v)H(W_i^{(2)}(v)) \tag{5.2}$$

for the damaged tissue. The superscripts 1 and 2 correspond to the normal and to the damaged tissue showing that the parameters of these equations are different (connectivity and response functions). Therefore, the solutions $u(x,t)$ and $v(x,t)$ are also different even if the initial conditions are the same, $u(x,0) = v(x,0)$ for $x \in \mathbb{R}$.

Consider, next, equation for the damaged tissue with an external stimulation $I(x,t)$:

$$\frac{\partial z}{\partial t} = D\frac{\partial^2 z}{\partial x^2} + g(K-z)H(W_a^{(2)}(z)) - g(z)H(W_i^{(2)}(z)) + I(x,t). \tag{5.3}$$

We are interested in the following question:

Is it possible to choose stimulation $I(x,t)$ in such a way that solution $z(x,t)$ of Equation 5.3 *becomes the same as solution $u(x,t)$ of Equation* 5.1?

If this is possible, then external stimulation can completely reconstruct wave propagation. In spite of the importance of this problem for the application, the solution of this seemingly difficult question is simple. Assuming that $z(x,t) = u(x,t)$, substitute the function $u(x,t)$ in Equation 5.3. Then we get

$$I(x,t) = \frac{\partial u}{\partial t} - g(K-u)H(W_a^{(2)}(u)) + g(u)H(W_i^{(2)}(u)) =$$

$$g(K-u)H(W_a^{(1)}(u)) - g(u)H(W_i^{(1)}(u)) - g(K-u)H(W_a^{(2)}(u)) + g(u)H(W_i^{(2)}(u)).$$

Thus, the stimulation function

$$I(x,t) = g(K-u)\left(H(W_a^{(1)}(u)) - H(W_a^{(2)}(u))\right) - g(u)\left(H(W_i^{(1)}(u)) - H(W_i^{(2)}(u))\right)$$

gives solution of the complete reconstruction problem. If we need to reconstruct the solution $u(x,t)$ not for all values of x, but only in one or several points x_i (electrodes), then different stimulation functions can provide such solution. In this case, we can also consider the problem of optimal control minimizing the total intensity of stimulation $\int_0^T \int_\Omega I^2(x,t)dxdt$.

6 | DISCUSSION

6.1 | Modeling

6.1.1 | Diffusion term in Equation 2.1

Neural field models are usually considered without the diffusion term.[37-40] From the mathematical point of view, introduction of the diffusion term is a generalization where the particular case $D = 0$ reduces it to the previous model. In Bessonov et al,[33] we showed that diffusion term influences the speed of wave propagation. In fact, there are two different regimes determined, respectively, by diffusion and by nonlocal interaction (connectivity function). If the diffusion coefficient is sufficiently large, then the wave speed is proportional to $\sqrt{D}$, as it is usually the case for reaction-diffusion waves. If the diffusion coefficient is small enough, then the wave speed becomes independent of it, and it is determined by the connectivity function. Hence, diffusion can influence wave propagation, and it can be useful to discuss its meaning in the neural field models.

The integral term in Equation 2.1 describes signal transmission between neurons along the axons. There are other possible mechanisms which can influence neuron activation. The first one is ion diffusion through the extracellular matrix which changes the distribution of electric potential and influences neuron activity. Assuming that the latter is proportional to the ionic concentrations, we naturally describe it by the diffusion term. Similar action can be produced by gap junction communication where neurons (and possibly glia cells) exchange ions directly and not through the extracellular matrix. Finally, another mechanism is related to the ephaptic effect[35] where neurons feel electric gradients from large groups of activated neurons through the extracellular matrix and respond to them. Diffusion term suggests a phenomenological description of this effect taking into account space transmission of neuron activation "from large to small" values.

6.1.2 | Connectivity and response functions

Connectivity functions are usually considered in the form of exponential functions with possibly different decaying rates for the activation and inhibition.[37] Nerve tissue is in general anisotropic with the length and density of axons possibly varying in space and according to their direction. The normal (orthodromic) direction of nerve impulse propagates from the soma towards the axon terminals. Therefore, the connectivity between the points x and y can differ from the connectivity between y and x. This difference signifies that the connectivity functions can be asymmetric, that is, their decay rate for positive and negative values of x can be different. Asymmetric connectivity functions are discussed in Pinotsis et al[38] on the basis of the experimental data.[45] Let us also note that antidromic impulse (direction opposite to normal) can be initiated by electric stimulation. It can be considered as an additional method of post-stroke stimulation.

The introduction of two different connectivity functions (activation, inhibition) and their possible asymmetry is essentially used in this work. Periodic spatial structures and waves emerge under certain relations between the two functions. It can be formulated as short range activation and long range inhibition. Surprisingly, this condition is similar to the condition of emergence of Turing structures in the activator-inhibitor models described by the reaction-diffusion systems of equations. This similarity allows us to suggest that this can be a general rule of the emergence of spatial structures which can be realized in different models.

Let us now discuss the role of two different response functions. If $S_a(u) \equiv S_i(u)$, then Equation 3.2 has typically three solutions: u_+, u_0, u_-, where u_+ and u_- are stable points and u_0 is unstable. Periodic spatial structures cannot bifurcate from the stable points since they lie on the "flat" parts of the sigmoid function, and the derivatives $S_a'(u_\pm)$ are small (cf Equation 3.7). The point u_0 cannot give rise to such structures neither because it is unstable. The situation becomes different in the case of different functions $S_a(u)$ and $S_i(u)$. Equation 3.2 can have a stable solution on growing branches of these functions (Figure A1).This point is stable if the slope of the inhibition response function is greater than the slope of the activation response function at the point of their intersection (we set here $\sigma = 0$ for simplicity).

Periodic spatial structures can be observed around solution $u = 0$ for a single response function $S_a(u) = S_i(u) = \arctan(hu)$ and $\phi_i^0 > \phi_a^0$ (Figure 1 and Appendix A). The linearized problem in this case is similar to the linearized problem with two different response functions and the solution u_- on the growing branch (Figure A1).

6.1.3 | Cortex waves and patterns

A large variety of waves and patterns are observed in neural field models. Among them stationary and oscillating Turing structures,[46] wave fronts,[47] periodic travelling waves (TW),[46,48-50] modulated waves,[46] pulses,[46,47,51] various two-dimensional patterns (see Kilpatrick and Bressloff[52] and the references therein). They are observed in all types of brain activities. These studies have various biological implications. Periodic waves propagation occur during language,[12,53-55] motor,[16] visual,[15] memory and spatial navigation[56] activities. In a review paper, Wu et al[57] examined propagating waves of activity within and between cortical areas during action, perception, or cognition. These authors suggest that TW are a manifestation of depolarization of the neuronal membrane. This depolarization increases the probability of firing action potentials in the population and these spikes will in turn depolarize more postsynaptic neurons in the neighboring area to sustain the propagation of the TW.[57] TW appear to subserve other functions as well. These authors suggest that "a sensory-evoked wave propagating to a larger area would increase the sensitivity/network gain for incoming stimulation. In this sense, the evoked wave generates an unintentional focus of attention in the sensory cortex. Furthermore, propagating waves associated with an oscillation can organize spatial phase distributions in a population of neurons." In a more recent review,[58] it was noted that cortical TW recorded at mesoscopic or macroscopic scales can be "spontaneously generated by recurrent circuits or evoked by external stimuli and travel along brain networks at multiple scales, transiently modulating spiking and excitability as they pass."

6.2 | Stimulation

We examine the situation of massive stroke at the chronic stage (6 months or more). Since the recent work of Rapela,[11,12] we know that when a subject produces consonant-vowel syllables, propagating waves are observed across the cortex. Rapela observed that during the production of traveling waves consonant-vowel syllables tend to propagate in the ventro-dorsal direction (ie, have negative speed). In addition, they tend to appear before the initiation of consonant-vowel syllables and disappear before their termination. In moments of silence, traveling waves tend to reverse direction and propagate in the dorso-ventral direction (ie, have positive speed) (see Figure 2; Rapela[12]). Below, we consider two scenarii in which the model could be useful.

6.2.1 | Scenario 1

In the first scenario, we consider that white matter connection is no-longer possible between two areas of convergence because of the presence of an ischemic core and a perilesional area surrounding this core zone (see Mandonnet and Duffau,[31] (figure 2)). One solution suggested by Mandonnet and Duffau[31] is to record in vPMC (ventral premotor cortex) and stimulate in vSMG (ventral supra marginal gyrus) to create a BCBI (brain computer brain interface) between these two areas. We propose instead to place the stimulator across the partially damaged but still functional ischemic zone and to use the model presented above (and in Bessonov et al[33] and Beuter et al[34]) to restore the parameters value of the propagating wave. Such an intervention could facilitate long-range communication disrupted in aphasia with only one grid of electrodes. The stimulator is used to record and stimulate at the cortical level in the perilesional area to recreate de bidirectional synchronized link (Figure 7).

6.2.2 | Scenario 2

In the second scenario, the ischemic zone is located in the vicinity of vSMG and information sent by vPMC can no longer be received in this zone. In this case, the stimulator is placed over the perilesional area. The traveling waves reach the perilesional zone and are recorded and analyzed before the same electrodes are used to stimulate the cortical tissue with parameters values modulated by the model. Again in this scenario, long range communication is facilitated (Figure 8).

How will the modulated stimulation be integrated with pathological activity? Part of the answer may come from a recent study by Voigt et al[59] using Intracortical Microstimulation (ICMS). In a different context, these authors wrote that "a low-current ICMS pulse modulated the way the auditory cortex processed a peripheral stimulus, by supra-additively combining the response to the ICMS with the cortical processing of the peripheral stimulus. This shows that the response to electrical stimulation is not substituting ongoing cortical activity but is integrated into the natural processes." Of course, the context in which we propose to use model-based stimulation to treat post-stroke aphasia is different.

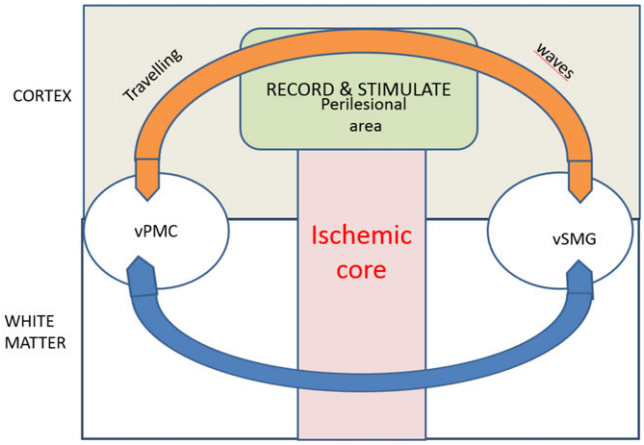

FIGURE 7 Schematic representation of scenario 1. In post-stroke aphasia we propose to restore long-range communication (interrupted by white matter ischemia) by reconnecting pre-identified areas which are still functional. Some electrodes are used to record activity coming from one area and the model is used to shape the stimulation pattern sent to the other area. Thus, as proposed by Mandonnet and Duffau[31] the bidirectional link between two areas can be restored but in this case using only one stimulator. vPMC, ventral premotor cortex; vSMG, ventral supra marginal gyrus [Colour figure can be viewed at wileyonlinelibrary.com]

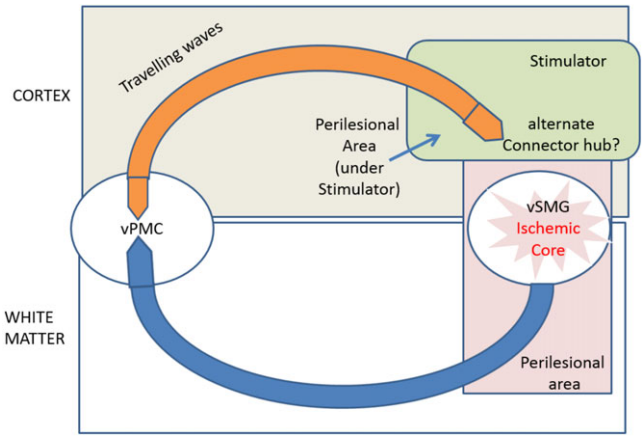

FIGURE 8 Schematic representation of scenario 2: In post-stroke aphasia, we propose to restore long-range communication (interrupted by white matter ischemia) by reconnecting two pre-identified areas which are still functional. Electrodes are used to record activity arriving from vPMC and the model is used to shape the stimulation pattern sent to the perilesional area of vSMG. Thus, as proposed by Mandonnet and Duffau,[31] the bidirectional link between the two areas can be restored but in this case using only one stimulator. vPMC, ventral premotor cortex; vSMG, ventral supra marginal gyrus. In this case, the alternate vSMG is progressively substituted to the original vSMG. This may be facilitated by combining neuromodulation and rehabilitation and if the treatment is successful the possibility to remove the electrode grid should be considered [Colour figure can be viewed at wileyonlinelibrary.com]

The proposed cortical stimulation could assist at least temporarily the damaged tissue. We do not exclude yet the possibility that after combining modulation of cortical waves with a rehabilitation program, the electrodes might be no longer needed. Although the model is proposed in the treatment of a specific condition (ie, post-stroke aphasia), it is generic.

7 | CONCLUSIONS AND PERSPECTIVES

Brain disorders are considered a major and growing health care problem today, notably because of the aging of the population.[60] Each year, more than 15 million people worldwide suffer from stroke,[61] and 1.1 million persons are affected in Europe,[62] often resulting in persisting handicaps such as language disorders[63] as well as cognitive, motor, and sensory impairments.[64]

Recovery can occur spontaneously but it can be amplified and accelerated by the use of noninvasive and invasive brain stimulation techniques. During the very late stage of recovery, improvements appear to reach a plateau in most patients but some patients continue to improve up to 25 years post-stroke.[65] Thus, there is a real need to explore how brain stimulation techniques could enhance remaining cortical excitability in the affected hemisphere[66] and accelerate late (or very late) phase recovery as nearly half of all stroke survivors require long-term care resulting in long-term high health care costs[18] and low quality of life.

The aim of the present paper was to study a theoretical model which explores the alteration of brain waves due to post-stroke cortical damage and show that, under specific conditions, cortical electrical stimulation could compensate for these deleterious effects. We discuss different stimulation methods and the conditions of their applicability. The theoretical studies show satisfactory results but the theory should be confirmed by the clinical proof of concept with the data from patients. A number of further steps will be required for the implementation of the stimulation technique, including data treatment and the development of the brain-computer interface. Additional studies will be required in order to determine optimal and efficient patient specific stimulation based on the closed-loop approach.

From the modeling perspective, there are various directions of the development of neural field models. Among them, let us mention fractional derivative models which are used to describe biological tissues including heart and brain.[67] Fractional derivatives with respect to time take into account memory and delay effects, and they provide a flexible modeling approach.[68] There is a vast literature devoted to nonlinear dynamics and numerical resolution of such models (see Hajipour et al[69,70] and the references therein) which can be used for further studies of neural field problems.

ACKNOWLEDGEMENTS

The work was partially supported by the "RUDN University Program 5-100," the RSF grant number 18-11-00171, and the French-Russian project PRC2307. There are no conflicts of interest to this work.

ORCID

Vitaly Volpert https://orcid.org/0000-0002-5323-9934

REFERENCES

1. Vosskuhl J, Strüber D, Herrmann CS. Non-invasive brain stimulation: a paradigm shift in understanding brain oscillations. *Front Hum Neurosci*. 2018;12:211. https://doi.org/10.3389/fnhum.2018.00211
2. Canavero S. Textbook of Therapeutic Cortical Stimulation (Versita/De Gruyter) Sergio Canavero (ed); 2015.
3. Dalise S, Ambrosio F, Modo M. Adaptive plasticity and recovery in preclinical models of stroke. *Arch Ital Biol*. 2014;152:190-215. https://doi.org/10.12871/00039829201442
4. Kiran S. What is the nature of poststroke language recovery and reorganization? *Int Sch Res Netw ISRN Neurol*. 2012;2012:786872. 13 pages https://doi.org/10.5402/2012/786872
5. Takeuchi N, Izumi S-I. Combinations of stroke neurorehabilitation to facilitate motor recovery: perspectives on Hebbian plasticity and homeostatic metaplasticity. *Front Hum Neurosci*. 2015;9:349. https://doi.org/10.3389/fnhum.2015.00349
6. Balossier A., Etard O., Descat C., Vivien D., Emery E.. Epidural cortical stimulation as a treatment for poststroke aphasia: a systematic review of the literature and underlying neurophysiological mechanisms. *Neurorehabil Neural Repair*. 2016;30(2):120-30. https://doi.org/10.1177/1545968315606989
7. Norise C, Hamilton RH. Non-invasive brain stimulation in the treatment of post-stroke and neurodegenerative aphasia: parallels, differences, and lessons learned. *Front Hum Neurosci*. 2017;10:675. https://doi.org/10.3389/fnhum.2016.00675
8. Sporns O. The human connectome: origins and challenges. *NeuroImage*. 2013;80:53-61. [PubMed: 23528922].
9. Kopell N, Gritton HJ, Whittington MA, Kramer MA. Beyond the connectome: the dynome. *Neuron*. 2014;83(6):1319-1328. https://doi.org/10.1016/j.neuron.2014.08.016
10. Zhang H, Watrous AJ, Patel A, Jacobs J. Theta and alpha oscillations are traveling waves in the human neocortex. *Neuron*. 2018;98:1-13. 2018 Elsevier Inc. https://doi.org/10.1016/j.neuron.2018.05
11. Rapela J. Rhythmic production of consonant-vowel syllables synchronizes traveling waves in speech-processing brain regions arXiv.org [q-bio] arXiv:1705.01615; 2017.
12. Rapela J. Traveling waves appear and disappear in unison with produced speech arXiv:1806.09559v1 [q-bio.NC] 25 Jun 2018; 2018.
13. Bahramisharif A, van Gerven MAJ, Aarnoutse EJ, et al. Propagating neocortical gamma bursts are coordinated by traveling alpha waves. *J Neurosci*. 2013;33(48):18849-18854.
14. Patten TM, Rennie CJ, Robinson PA, Gong P. Human cortical traveling waves: d properties and correlations with responses. *PLoS ONE*. 2012;7(6):e38392.

15. Sato TK, Nauhaus I, Carandini M. Traveling waves in visual cortex. *Neuron*. 2012;75:218-229.
16. Takahashi K, Kim S, Coleman TP, et al. Large-scale spatiotemporal spike patterning consistent with wave propagation in motor cortex. *Nat Commun*. 2015;6:7169.
17. Tang E, Bassett DS. Control of dynamics in brain networks. *Rev Mod Phys*. 2018;90: 031003.
18. Azad TD, Anand Veeravagu BA, Steinberg GK. Neurorestoration after stroke. *Neurosurg Focus*. 2016;40(5):E2. https://doi.org/10.3171/2016.2.FOCUS15637
19. Hatem SM, Saussez G, della Faille M, et al. Rehabilitation of motor function after stroke: a multiple systematic review focused on techniques to stimulate upper extremity recovery. *Front Hum Neurosci*. 2016;10:442. https://doi.org/10.3389/fnhum.2016.00442
20. Levy RM, Harvey RL, Kissela BM, et al. Epidural electrical stimulation for stroke rehabilitation: results of the prospective, multicenter, randomized, single-blinded everest trial. *Neurorehabil Neural Repair*. 2016;30(2):107-119. https://doi.org/10.1177/1545968315575613
21. LoPresti MA, Camacho E, Appelboom G, Connolly ESJr. The promising role of neuromodulation in improving ischemic stroke recovery. *J Neurol Neurg*. 2015;1(2):112.
22. Plow EB, Carey JR, Nudo RJ, Pascual-Leone A. Invasive cortical stimulation to promote recovery of function after stroke: a critical appraisal. *Stroke*. 2009;40:1926-31.
23. Wessel MJ, Zimerman M, Hummel FC. Non-invasive brain stimulation: an interventional tool for enhancing behavioral training after stroke. *Front Hum Neurosci*. 2015;9:265. https://doi.org/10.3389/fnhum.2015.00265
24. Kubis N. Non-invasive brain stimulation to enhance post-stroke recovery. *Front Neural Circuits*. 2016;10:56. https://doi.org/10.3389/fncir.2016.00056
25. Cherney LR. Epidural cortical stimulation as adjunctive treatment for nonfluent aphasia: Phase 1 clinical trial follow-up findings. *Neurorehabil Neural Repair*. 2016;30(2):131-142.
26. Meinzer M, Darkow R, Lindenberg R, Floel A. Electrical stimulation of the motor cortex enhances treatment outcome in post-stroke aphasia. *Brain J Neurol*. 2016;139:1152-63.
27. Mohr B. Neuroplasticity and functional recovery after intensive language therapy in chronic post stroke aphasia: which factors are relevant? *Front Hum Neurosci*. 2017;11:332. https://doi.org/10.3389/fnhum.2017.00332
28. Santos MD, Cavenaghi VB, Mac-Kay APMG, et al. Non-invasive brain stimulation and computational models in post-stroke aphasic patients: single session of transcranial magnetic stimulation and transcranial direct current stimulation. A randomized clinical trial. *Sao Paulo Med J*. 2017;135(5):475-80. https://doi.org/10.1590/1516-3180.2016.0194060617
29. Shah PP, Szaflarski JP, Allendorfer J, Hamilton RH. Induction of neuroplasticity and recovery in post-stroke aphasia by non-invasive brain stimulation. *Front Hum Neurosci*. 2013;7:888. https://doi.org/10.3389/fnhum.2013.00888
30. Spelmann K, Van de Sandt-Koenderman WME, Heijenbrok-Kal MH, Ribbers GM. Comparison of two configurations of transcranial direct current stimulation for treatment of aphasia. *J Rehabil Med*. 2018;50:527-533. https://doi.org/10.2340/16501977-2338
31. Mandonnet E, Duffau H. Understanding entangled cerebral networks: a prerequisite for restoring brain function with brain-computer interfaces. *Front Syst Neurosci*. 2014;8:82. https://doi.org/10.3389/fnsys.2014.00082
32. To WT, De Ridder D, Hart JJr, Vanneste S. Changing brain networks through non-invasive neuromodulation. *Front Hum Neurosci*. 2018;12:128. https://doi.org/10.3389/fnhum.2018.00128
33. Bessonov N, Beuter A, Trofimchuk S, Volpert V. Estimate of the travelling wave speed for an integro-differential equation. *Appl Math Lett*. 2018;88:103-110. https://doi.org/10.1016/j.aml.2018.07.037
34. Beuter A, Balossier A, Trofimchuk S, Volpert V. Modeling Of post-stroke stimulation of cortical tissue. *Math Biosci*. 2018;305:146-159. https://doi.org/10.1016/j.mbs.2018.08.014
35. Buzsaki G, Anastassiou CA, Koch C. The origin of extracellular fields and currents EEG, ECoG, LFP and spikes. *Nat Rev Neurosci*. 2016;13(6):407-420.
36. Wilson HR, Cowan JD. A mathematical theory of the functional dynamics of cortical and thalamic nervous tissue. *Kybernetik*. 1973;13:55-80.
37. Modolo J, Bhattacharya B, Edwards R, Campagnaud J, Legros A, Beuter A. Using a virtual cortical module implementing a neural field model to modulate brain rhythms in Parkinson's disease. *Front Neurosci*. 2010;4:45.
38. Pinotsis DA, Hansen E, Friston KJ, Jirsa VK. *Anatomical connectivity and the resting state activity of large cortical networks Neuroimage*. 2013;65:127-138.
39. Ermentrout B, McLeod JB. Existence and uniqueness of travelling waves for a neural network. *Proc Roy Soc Edinburgh*. 1994;134A:1013-1022.
40. Chen Z, Ermentrout B, Wang XJ. Wave propagation mediated by GABAB synapse and rebound excitation in an inhibitory network: a reduced model approach. *J Comput Neurosci*. 1998;5:53-69.
41. Volpert V. *Elliptic Partial Differential Equations Volume 2. Reaction-diffusion equations*. Basel: Birkhauser; 2014.
42. Chen X. Existence, uniqueness, and asymptotic stability of travelling waves in nonlocal evolution equations. *Adv Differ Equ*. 1997;2:125-160.
43. Ducrot A, Marion M, Volpert V. Spectrum of some integro-differential operators and stability of travelling waves. *Nonlinear Anal Ser A Theory Methods Appl*. 2011;74(13):4455-4473.
44. Ma S, Wu J. Existence, uniqueness and asymptotic stability of traveling wavefronts in a non-local delayed diffusion equation. *J Dyn Diff Equat*. 2007;19(2):391-436.

45. Stephan KE, Kamper L, Bozkurt A, Burns GAP, Young MP, Kötter R. Advanced database methodology for the collation of connectivity data on the Macaque brain (CoCoMac). *Philos Trans R Soc London Ser B Biol Sci*. 2001;356:1159-1186.
46. Venkov NA, Coombes S, Matthews PC. Dynamic instabilities in scalar neural field equations with space-dependent delays. *Phys D*. 2007;232:1-15.
47. Pinto DJ, Ermentrout GB. Spatially structured activity in synaptically coupled neuronal networks: I. Travelling fronts and pulses. *SIAM J Appl Math*. 2001;62(1):206-225.
48. Atay FM, Hutt A. Neural fields with distributed transmission speeds and long-range feedback delays. *SIAM J Appl Dyn Syst*. 2006;5(4):670-698.
49. Meijer HGE, Coombes S. Travelling waves in a neural field model with refractoriness. *J Math Biol*. 2014;68:1249-1268.
50. Senk J, Korvasova K, Schuecker J, et al. Conditions for traveling waves in spiking neural networks. arXiv.org > q-bio > arXiv:1801.06046v1.
51. Pinto DJ, Ermentrout GB. Spatially structured activity in synaptically coupled neuronal networks: II. Lateral inhibition and standing pulses. *SIAM J Appl Math*. 2001;62(1):226-243.
52. Kilpatrick ZP, Bressloff PC. Spatially structured oscillations in a two-dimensional excitatory neuronal network with synaptic depression. *J Comput Neurosci*. 2010;28:193-209.
53. Gross J, Hoogenboom N, Thut G, et al. Speech rhythms and multiplexed oscillatory sensory coding in the human brain. *PLoS Biol*. 2013;11(12):e1001752. https://doi.org/10.1371/journal.pbio.1001752
54. Weaver J. How brain waves help us make sense of speech. *PLoS Biol*. 2013;11(12):e1001753. https://doi.org/10.1371/journal.pbio.1001753
55. Botella-Soler V, Valderrama M, Crépon B, Navarro V, Le Van Quyen M. Large-Scale Cortical dynamics of sleep slow waves. *PLoS ONE*. 2012;7(2):e30757. https://doi.org/10.1371/journal.pone.0030757
56. Zhang H, Jacobs J. Traveling Theta Waves in the Human Hippocampus. *J Neurosci*. 2015;35(36):12477-12487.
57. Wu JY, Huang X, Zhang C. Propagating waves of activity in the neocortex: What they are, what they do. *Neuroscientist*. 2008;14(5):487-502.
58. Muller L, Chavane F, Reynolds J, Sejnowski TJ. Cortical travelling waves: mechanisms and computational principles. *Nat Rev Neurosci*. 2018;19(5):255-268. https://doi.org/10.1038/nrn.2018.20
59. Voigt MB, Yusuf PA, Kral A. Intracortical Microstimulation Modulates Cortical Induced Responses. *Journal of Neuroscience*. 2018;38(36):7774-7786. https://doi.org/10.1523/JNEUROSCI.0928-18.2018
60. Dickey L, Kagan A, Lindsay MP, Fang J, Rowland A, Black S. Incidence and profile of inpatient stroke-induced aphasia in ontario. *Canada Arch Phys Med Rehabil*. 2010;91:196-202.
61. Feigin VL, Forouzanfar MH, Krishnamurthi R, et al. Global and regional burden of stroke during 1990–2010: Findings from the global burden of disease study 2010. *Lancet*. 2014;18:245-254. 383(9913).
62. Béjot Y, Bailly H, Durier J, Giroud M. Epidemiology of stroke in europe and trends for the 21st century. *Presse Med*. 2016;45:e391-e398. https://doi.org/10.1016/j.lpm.2016.10.003 (12 Pt 2):e391-e398 Epub 2016 Nov 2.
63. Laska AC, Hellblom A, Murray V, Kahan T, Arbin MV. Aphasia in acute stroke and relation to outcome. *J Intern Med*. 2001;249:413-422.
64. Gardner MJ, Ong BC, Liporace F, Koval KJ. Orthopedic issues after cerebrovascular accident. *Am J Orthop*. 2002;31:559-568.
65. Smania N, Gandolfi M, Aglioti S, Girardi P, Fiaschi A, Girardi F. How long is the recovery of global aphasia? Twenty-five years of follow-up in a patient with left hemisphere stroke. *Neurorehabil Neural Repair*. 2010;24(9):871-875.
66. Carmichael ST. Brain excitability in stroke: The yin and yang of stroke progression. *Arch Neurol*. 2012;69:161167. https://doi.org/10.1001/archneurol.2011.1175
67. Magin RL. Fractional calculus models of complex dynamics in biological tissues. *Comput Math Appl*. 2010;59:1586-1593.
68. Jajarmi A, Baleanu D. A new fractional analysis on the interaction of HIV with CD4 + T-cells. *Chaos, Solitons Fractals*. 2018;113:221-229.
69. Hajipour M, Jajarmi A, Baleanu D, Sun H. On an accurate discretization of a variable-order fractional reaction-diffusion equation. *Commun Nonlinear Sci Numer Simulat*. 2019;69:119-133.
70. Hajipour M, Jajarmi A, Baleanu D. On the nonlinear dynamical systems within the generalized fractional derivatives with mittag–leffler kernel. *Nonlinear Dyn*. 2018;94:397-414.

APPENDIX A: FUNCTIONS AND PARAMETERS

A.1 | Response functions.

Typical sigmoid functions are shown in Figure A1:

$$S_a(u) = \frac{e^{2x-5}}{1+e^{2x-5}}\ , \qquad S_a(u) = \frac{e^{5x-12.5}}{1+e^{5x-12.5}}\ .$$

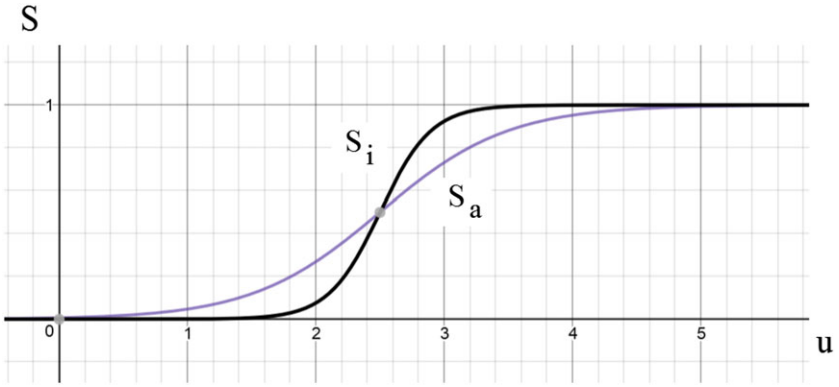

FIGURE A1 Qualitative representation of the activating S_a and inhibitory S_i response functions [Colour figure can be viewed at wileyonlinelibrary.com]

A.2 | Figure 1.

Functions:

$$\sigma_1(\xi) = 20\left(\frac{8}{400+\xi^2} - \frac{2}{100+\xi^2}\right) - 10^{-4}\xi^2$$

(solid line),

$$\sigma_2(\xi) = 20\left(\frac{4.5}{400+\xi^2} - \frac{2}{100+\xi^2}\right) - 10^{-4}\xi^2$$

(dashed line). Values of parameters: $a_1 = 0.2, a_2 = 0.1, a_3 = 0.2, a_4 = 0.1, b_1 = 20, b_2 = 10, b_3 = 20, b_4 = 10, D = 10^{-4}, h = 20, L = 2, N = 401$; $S(u) = \arctan(hu)$.

A.3 | Figure 2.

Values of parameters: $a_2 = 0.1, a_4 = 0.1, b_1 = 20, b_2 = 10, b_3 = 20, b_4 = 10, D = 10^{-4}, h = 20, L = 2, N = 401$; $S(u) = \arctan(hu)$, σ is varied (bifurcation parameter);

A.4 | Figure 3.

Values of parameters for the left figure: $a_1 = 1, a_2 = 0, a_3 = 1, a_4 = 0, b_1 = 40, b_2 = 10, b_3 = 40, b_4 = 10, D = 10^{-4}, \sigma = 0.1, h = 20, L = 10, N = 1001$; $S(u) = \arctan(hu)$.

Values of parameters for the right figure: $a_1 = 1, a_2 = 1, a_3 = 1, a_4 = 1, b_1 = 40, b_2 = 10, b_3 = 40, b_4 = 10, D = 10^{-4}, \sigma = 0.1, h = 20, L = 10, N = 1001$; $S(u) = \arctan(hu)$.

A.5 | Figure 4.

Values of parameters: $a_1 = 0.5, a_2 = 0.1, a_3 = 0.1, a_4 = 0.1, b_1 = 20, b_2 = 10, b_3 = 20, b_4 = 10, D = 10^{-4}, \sigma = 0.08, h = 20, L = 2, N = 401$; $S(u) = \arctan(hu)$.

A.6 | Figure 5.

Values of parameters for the left figure: $a_1 = 0.9, a_2 = 0.9, a_3 = 4, a_4 = 4, b_1 = 40, b_2 = 20, b_3 = 40, b_4 = 20, D = 10^{-4}, \sigma = 0.01, h = 20, L = 2, N = 401$; $S(u) = \arctan(hu)$.

Values of parameters for the right figure: $a_1 = 0.5, a_2 = 0.5, a_3 = 4, a_4 = 4, b_1 = 40, b_2 = 20, b_3 = 40, b_4 = 20, D = 10^{-4}, \sigma = 0.01, h = 20, L = 2, N = 401$; $S(u) = \arctan(hu)$.

A.7 Figure 6.

Values of parameters: $a_1 = 0.4, a_2 = 0.1, a_3 = 0.4, a_4 = 0.1, b_1 = 40, b_2 = 10, b_3 = 40, b_4 = 10, D = 10^{-4}, \sigma = 0.1, h = 20, L = 2, N = 401, p = -10, q = 0.2, I_0 = 0.5$; $S(u) = \arctan(hu)$.